International Journal of Computational Methods
Vol. 9, No. 1 (2012) 1240007 (13 pages)

DOI: 10.1142/S0219876212400075

AN ADAPTIVE TIME-STEPPING PROCEDURE BASED ON THE SCALED BOUNDARY FINITE ELEMENT METHOD FOR ELASTODYNAMICS

Z. H. ZHANG
College of Civil Engineering and Architecture
Zhejiang University, Hangzhou, 310058, China
zhangzihua1984@gmail.com

Z. J. YANG*
School of Engineering, The University of Liverpool
Liverpool, L69 3GQ, UK
**zhenjun.yang@liverpool.ac.uk*

GUOHUA LIU
College of Civil Engineering and Architecture
Zhejiang University, Hangzhou, 310058, China
zjuliu@163.com

Received 20 November 2010
Accepted 3 March 2011

This study develops an adaptive time-stepping procedure of Newmark integration scheme for transient elastodynamic problems, based on the semi-analytical scaled boundary finite element method (SBFEM). In each time step, *a posteriori* local error estimator based on the linear distributed acceleration is employed to estimate the error caused by the time discretization. The total energy of the domain, consisting of the kinetic energy and the strain energy, is calculated semi-analytically. The time increment is automatically adjusted according to a simple criterion. Three examples with stress wave propagation were modeled. The numerical results show that the developed method is capable of limiting the local error estimator within specified targets by using an optimal time increment in each time step.

Keywords: Scaled boundary finite element method; time adaptivity; elastodynamics; Newmark integration method; local error estimator.

1. Introduction

In elastodynamic problems with stress wave propagation, the discretization error of numerical methods is caused by two sources: the spatial discretization and the time

*Corresponding author.

discretization. The spatial discretization error can be limited by spatially adaptive techniques, such as h-adaptive method [Zeng and Wiberg (1992a)], based on the identification of steep stress regions. Even if an optimal mesh is identified in each time step or a very fine mesh is used constantly, the adaptive procedure of the time increment, termed adaptive time-stepping procedure herein, is still very important. For example, in some practical geotechnical problems, the dynamic process may be very rapid in some time intervals but slow in others. As a result, it is inefficient and impractical to use a constant time increment in the whole process. In order to improve computing efficiency, adaptive time-stepping procedures based on local error estimations have been developed in finite element method (FEM). Zienkiewicz and Xie [1991] proposed a local error estimator by comparing the solutions from the Newmark integration method and exact solutions from the Taylor expansion. Zeng *et al.* [1992c] obtained the same estimator in a more intuitive way and demonstrated that the estimator converged asymptotically to the exact local error by modeling a single degree of freedom (DOF) example. However, this estimator only considers the errors of displacements. Li *et al.* [1993] took into account the errors of both displacements and velocities and established more accurate and complete local error estimators. However, for large-scale problems [Voleti *et al.* (1996)] and high-frequency dynamic problems [Ihlenburg *et al.* (1997)], a large number of DOFs are required in FEM, leading to high computational cost.

The scaled boundary finite element method (SBFEM), developed by Song and Wolf in 1990s [Wolf and Song (1997)], is a semi-analytical method combining the advantages of FEM and the boundary element method (BEM). It discretizes subdomain boundaries only and thus the modeling dimensions are reduced by one as the BEM, but no fundamental solutions are needed. As a result, only a small number of DOFs are needed for typical elastic problems. These features often lead to higher computational efficiency and accuracy than traditional FEM, especially for problems with stress singularity [Yang (2006); Yang *et al.* (2007)]. Adaptive scaled boundary finite element method (ASBFEM) based procedures have been devised recently for static problems to control the spatial discretization error [Deeks and Wolf 2002a,b], where the superconvergent patch recovery technique and the *a posteriori* error estimator developed by Zienkiewicz and Zhu [1987] for FEM were extended to SBFEM with h-refinement. More recently, the authors developed an h-hierarchical ASBFEM procedure for general elastodynamic problems [Yang *et al.* (2011)]. However, very small constant time increments were used to avoid the time discretization error. These studies demonstrate that the ASBFEM is significantly more efficient than adaptive FEM.

This study extends the local error estimator proposed by Zeng *et al.* [1992c] to the SBFEM, to control the time discretization error and improve computational accuracy and efficiency for modeling elastodynamic problems. Three examples were modeled to demonstrate the effectiveness and efficiency of the developed time-stepping procedure.

2. Methodology

2.1. *The scaled boundary FEM*

A domain of arbitrary shape is illustrated in Fig. 1(a) as an example. The domain is divided into three subdomains. Any scheme of subdivision, with various numbers, shapes, and sizes of subdomains, can be used, as long as a scaling center for each subdomain can be found from which the subdomain boundary is fully visible. Figure 1(b) shows the details of Subdomain 1. The subdomain is represented by scaling a defining curve S relative to a scaling center. The defining curve is usually taken to be the domain boundary, or part of the boundary. A normalized radial coordinate ξ is defined, varying from zero at the scaling center and unit value on S. A circumferential coordinate η is defined along the defining curve S. A curve similar to S defined by $\xi = 0.5$ is shown in Fig. 1(b). The coordinates ξ and η form the local coordinate system used in all subdomains.

The basic assumption of the SBFEM is that the displacement field in a subdomain is

$$\mathbf{u}(\xi, \eta) = \mathbf{N}(\eta)\mathbf{u}(\xi), \tag{1}$$

where $\mathbf{N}(\eta)$ is the shape function matrix in the circumferential direction, which is the same as used in FEM, and $\mathbf{u}(\xi)$ denotes the displacements along the radial lines, which are analytical with respect to the radial coordinate ξ.

2.2. *Solutions in the time domain*

Starting from the virtual work principle and using the Newmark integration method, Yang *et al.* [2011] have derived displacement, velocity, and acceleration fields in

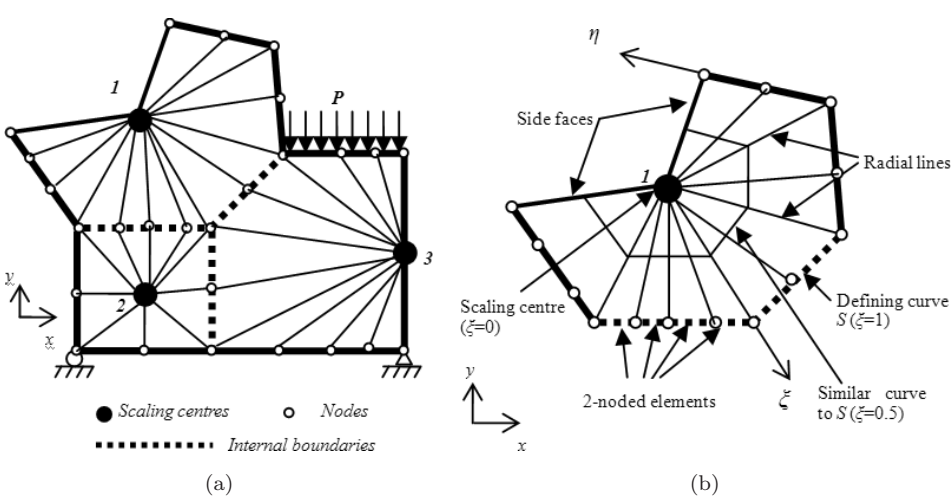

Fig. 1. The concept of the SBFEM: (a) subdomaining of a domain and (b) subdomain 1.

subdomains as:

$$\mathbf{u}(\xi,\eta) = \mathbf{N}(\eta)\sum_{i=1}^{N} c_i \xi^{\lambda_i}\boldsymbol{\varphi}_i, \quad \dot{\mathbf{u}}(\xi,\eta) = \mathbf{N}(\eta)\sum_{i=1}^{N} \dot{c}_i \xi^{\lambda_i}\boldsymbol{\varphi}_i,$$
$$\ddot{\mathbf{u}}(\xi,\eta) = \mathbf{N}(\eta)\sum_{i=1}^{N} \ddot{c}_i \xi^{\lambda_i}\boldsymbol{\varphi}_i, \tag{2}$$

where N is the DOFs of the subdomain and λ_i and $\boldsymbol{\varphi}_i$ are the N number of positive eigenvalues and corresponding eigenvectors (modal displacements) of a standard eigenproblem. They can be interpreted as independent deformation modes that closely satisfy internal equilibrium in the ξ direction. $\dot{c}_i$ and $\ddot{c}_i$ are constants depending on boundary conditions. The stress field in the subdomain is calculated by

$$\boldsymbol{\sigma}(\xi,\eta) = \mathbf{D}\mathbf{B}^1(\eta)\left(\sum_{i=1}^{N} c_i\lambda_i\xi^{\lambda_i-1}\boldsymbol{\varphi}_i\right) + \mathbf{B}^2(\eta)\left(\sum_{i=1}^{N} c_i\xi^{\lambda_i-1}\boldsymbol{\varphi}_i\right) = \sum_{i=1}^{N} c_i\xi^{\lambda_i-1}\boldsymbol{\psi}_i, \tag{3}$$

where $\mathbf{D}$ is the material elasticity matrix, $\mathbf{B}^1$ and $\mathbf{B}^2$ are coefficient matrices dependent only on the boundary definition, and $\boldsymbol{\psi}_i$ is the ith stress mode.

It can be seen from Eqs. (2) and (3) that the displacement, velocity, acceleration, and stress fields in a subdomain are all analytical with respect to the radial coordinate ξ and approximate in FEM sense in the circumferential direction η.

2.3. *The local error estimator*

The original Newmark scheme, also called the *constant-average-acceleration method*, assumes that the acceleration in each time step is a constant equal to the average of accelerations at the two ends of the time step [Thomas and Gladwell (1988)], i.e. $(\ddot{\mathbf{U}}_t + \ddot{\mathbf{U}}_{t+\Delta t})/2$ in the time interval $[t, t+\Delta t]$ as illustrated in Fig. 2. This assumption leads to a discontinuous acceleration history.

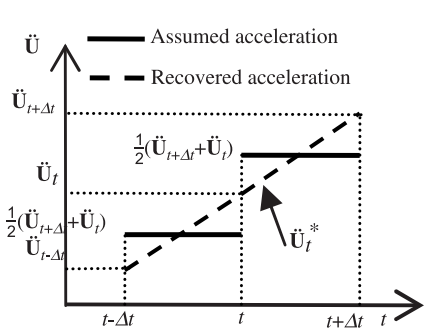

Fig. 2. Acceleration distributions.

To improve accuracy, Zeng *et al.* [1992c] assumed a continuous linear distribution of acceleration (the dash line in Fig. 2) as the recovered acceleration.

$$\ddot{\mathbf{U}}^* = \frac{\ddot{\mathbf{U}}_{t+\Delta t} - \ddot{\mathbf{U}}_t}{\Delta t}(\tau - t) + \ddot{\mathbf{U}}_t, \tag{4}$$

where $\tau \in [t, t + \Delta t]$. The acceleration error at time τ is estimated by

$$\ddot{\mathbf{e}}(\tau) \approx \frac{1}{2}(\ddot{\mathbf{U}}_{t+\Delta t} + \ddot{\mathbf{U}}_t) - \ddot{\mathbf{U}}^* = -\frac{\ddot{\mathbf{U}}_{t+\Delta t} - \ddot{\mathbf{U}}_t}{\Delta t}(\tau - t) + \frac{1}{2}(\ddot{\mathbf{U}}_{t+\Delta t} - \ddot{\mathbf{U}}_t). \tag{5}$$

Assuming the solutions at time t are exact, the velocity error at time τ is estimated by one-time integration of Eq. (5)

$$\dot{\mathbf{e}}(\tau) = \int_t^\tau \ddot{\mathbf{e}}(\tau')\mathrm{d}\tau' \approx -\frac{\ddot{\mathbf{U}}_{t+\Delta t} - \ddot{\mathbf{U}}_t}{2\Delta t}(\tau - t)^2 + \frac{1}{2}(\ddot{\mathbf{U}}_{t+\Delta t} - \ddot{\mathbf{U}}_t)(\tau - t). \tag{6}$$

The displacement error is then calculated by

$$\mathbf{e}(t + \Delta t) = \int_t^{t+\Delta t} \dot{\mathbf{e}}(\tau)\mathrm{d}\tau \approx \frac{1}{12}\Delta t^2(\ddot{\mathbf{U}}_{t+\Delta t} - \ddot{\mathbf{U}}_t). \tag{7}$$

A posteriori local error is finally obtained in the strain energy norm

$$\|\mathbf{e}\| = \sqrt{\mathbf{e}^T\mathbf{K}\mathbf{e}} \approx \frac{1}{12}\Delta t^2[(\ddot{\mathbf{U}}_{t+\Delta t} - \ddot{\mathbf{U}}_t)^T\mathbf{K}(\ddot{\mathbf{U}}_{t+\Delta t} - \ddot{\mathbf{U}}_t)]^{1/2}, \tag{8}$$

where $\mathbf{K}$ is the global stiffness matrix. The Newmark integration scheme with $\beta = 0.25$ is used in the above derivation. Other values of β can also be used.

In most cases, it is difficult to specify an absolute error tolerance of $\|\mathbf{e}\|$ and an error estimator relative to the total energy of the domain is usually used. The total energy of a domain can be calculated semi-analytically as [Yang *et al.* (2011)]:

$$\|\mathbf{u}\| = \left(\sum_{s=1}^{NS}\sum_{i=1}^{N}\sum_{j=1}^{N}\left(\frac{\rho\dot{c}_i\dot{c}_j}{\lambda_i + \lambda_j + 2}\int_{S_s}(\dot{\mathbf{u}}_i(\eta))^T\dot{\mathbf{u}}_i(\eta)|J|\mathrm{d}\eta \right.\right.$$
$$\left.\left. + \frac{c_ic_j}{\lambda_i + \lambda_j}\int_{S_s}\boldsymbol{\sigma}_i(\eta)^T\mathbf{D}^{-1}\boldsymbol{\sigma}_j(\eta)|J|\mathrm{d}\eta\right)\right)^{1/2} \tag{9}$$

where NS is the number of subdomains and ρ is the material density. $|J|$ is the determinant of Jacobian matrix, $\dot{\mathbf{u}}_i(\eta)$ the ith mode of velocity, and $\boldsymbol{\sigma}_i(\eta)$ the ith mode of stress on the subdomain boundary S_s, respectively.

The relative local error estimator is defined as:

$$\omega = \frac{\|\mathbf{e}\|}{\|\mathbf{u}\|} \times 100\%. \tag{10}$$

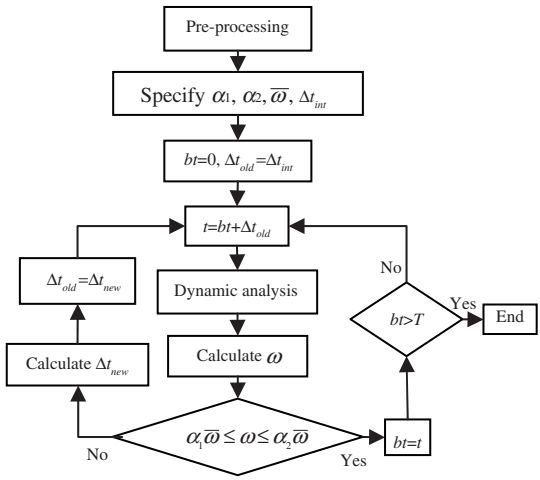

Fig. 3. The flowchart of the adaptive time-stepping procedure.

3. The Time Adaptive Procedure

The aim of the time adaptive procedure is to adjust the time increment, so that the local error estimator is controlled within a target range for each time step [Zeng *et al.* (1992c)]

$$\alpha_1\bar{\omega} \le \omega \le \alpha_2\bar{\omega}, \tag{11}$$

where $\bar{\omega}$ is the target error estimator, $0 \le \alpha_1 \le 1$ and $\alpha_2 \ge 1$ are two limiting parameters.

If the inequality (11) is not satisfied, the time increment is adjusted according to

$$\Delta t_{\text{new}} = \left(\frac{\bar{\omega}}{\omega}\right)^{1/3} \Delta t_{\text{old}}, \tag{12}$$

where Δt_{new} is the new time increment after adjustment and Δt_{old} is the optimal time increment identified in the previous time step.

Figure 3 illustrates a simple flowchart of the adaptive time-stepping procedure.

4. Numerical Examples

Three examples were modeled to validate the developed method. The following parameters are used for all the examples: $\bar{\omega} = 1\%$, $\alpha_1 = 0.9$, $\alpha_2 = 1.1$, and $\Delta t_{\text{int}} = 0.01\,\text{s}$.

4.1. *Example 1: An* L*-shaped domain under blast*

The first example is an L-shaped domain subjected to a triangular blast-like loading (Fig. 4). Dynamic responses in a time period of (0.0, 8.0 s) were calculated.

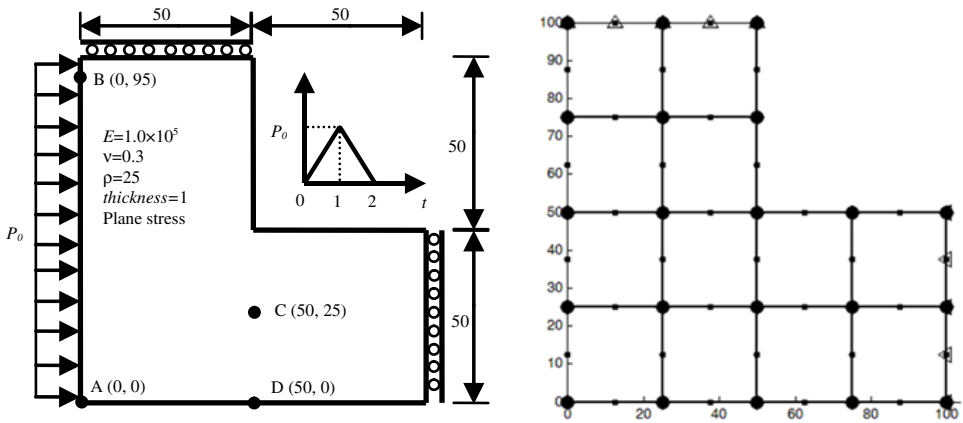

Fig. 4. Example 1: an L-shaped domain and its mesh (DOFs = 106).

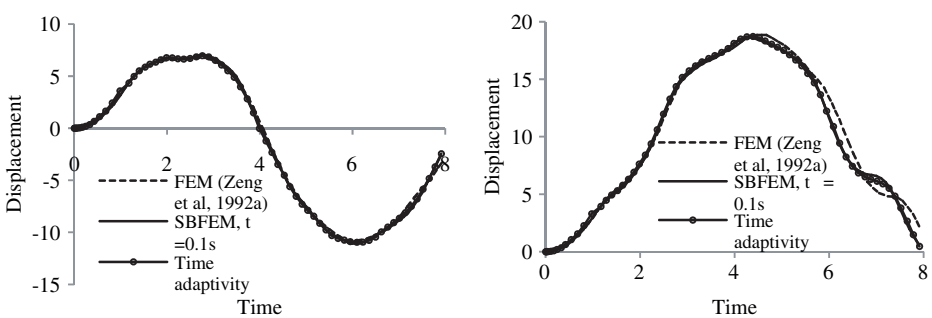

(a) Point A (b) Point B

Fig. 5. Histories of horizontal displacement of points A and B.

Figures 5 and 6 show the displacement and stress responses at points A, B, C, and D. It can be seen that the results of the time adaptive method agree very well with the nonadaptive SBFEM, which used a uniform time increment $\Delta t = 0.1\,\mathrm{s}$. The results from FEM using 4,554 DOFs [Zeng and Wiberg (1992a)] are also plotted for comparison.

Figure 7(a) shows the histories of the local error estimator using the SBFEM with and without time adaptivity. For nonadaptive SBFEM, the error estimator fluctuates around 3% for uniform $\Delta t = 0.2\,\mathrm{s}$. For $\Delta t = 0.1\,\mathrm{s}$, the estimator is less than 1% in most time steps, but it is high at the initial stage. The present method is able to control the error estimator closely around 1% during the whole process. Figure 7(b) shows the time increment history used in the adaptive SBFEM. It is clear that the time increment is adapted according to Eq. (12). In particular, very short time increments are used at the beginning to reduce error.

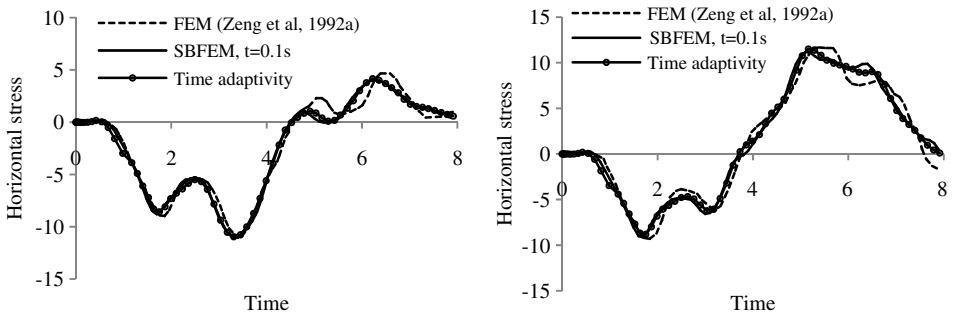

(a) Point C (b) Point D

Fig. 6. Histories of horizontal stress of points C and D.

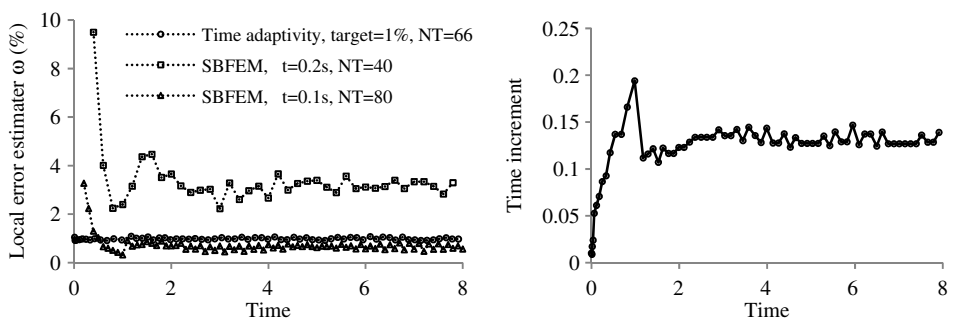

(a) (b)

Fig. 7. Histories of the local error estimator and the time increment used for Example 1: (a) the local error estimator and (b) the time increment.

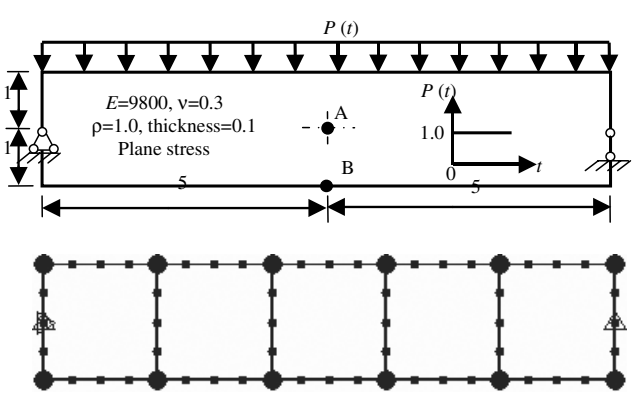

Fig. 8. Example 2: a simply supported beam and the mesh (DOFs = 120).

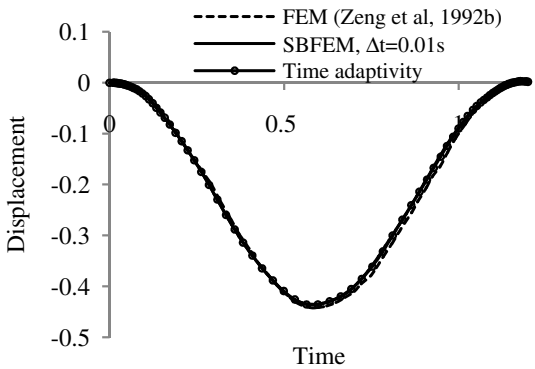

Fig. 9. Histories of vertical displacement of point A.

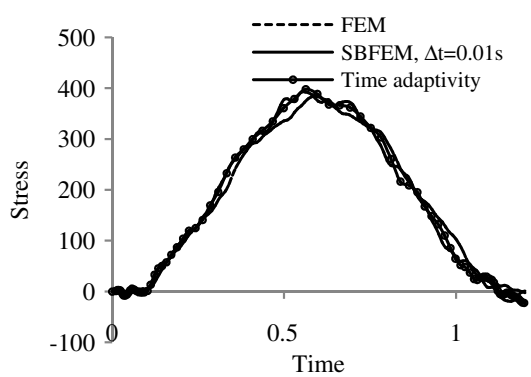

Fig. 10. Histories of horizontal stress of point B.

4.2. *Example 2: A simply supported beam under impact*

A simply supported beam subjected to a uniformly distributed loading in the form of Heaviside function on the beam top face. The dimensions, material properties, and mesh are shown in Fig. 8. The dynamic responses in a time period of (0, 1.2 s) were calculated.

Figure 9 shows the vertical displacement histories at point A, calculated by the present method, nonadaptive SBFEM, and FEM using 2909 DOFs [Zeng *et al.* (1992b)], respectively. Almost the same results were predicted from the nonadaptive SBFEM and the present method and they are also close to those of FEM. Figure 10 compares favorably the horizontal normal stresses at point B from the three methods.

Figure 11(a) shows the histories of the local error estimator in present method and nonadaptive SBFEM with constant time increments $\Delta t = 0.01$ s and $\Delta t = 0.02$ s, respectively. It can be seen that the local error estimator from nonadaptive

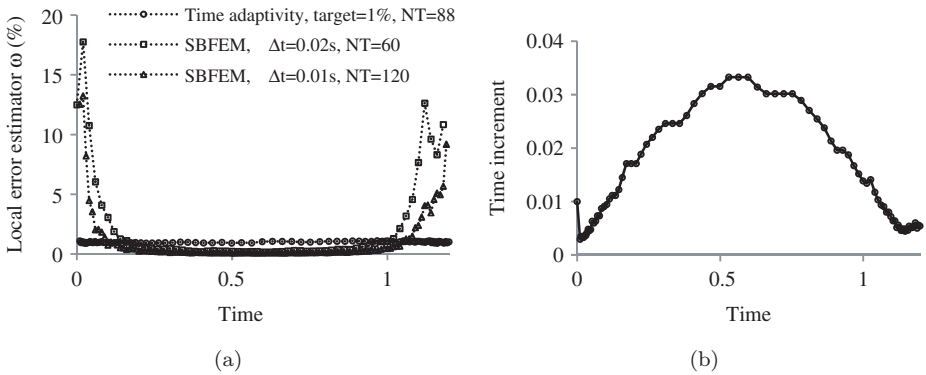

Fig. 11. Histories of the local error estimator and the time increment used for Example 2: (a) the local error estimator and (b) the time increment.

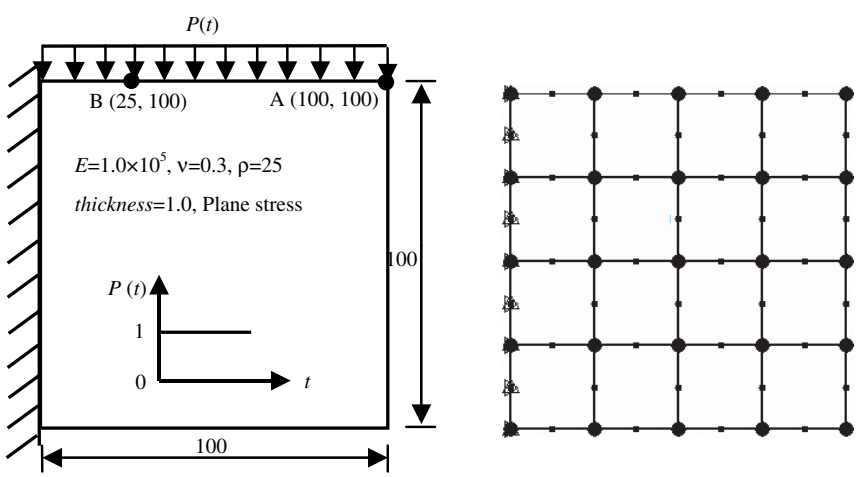

Fig. 12. Example 3: a deep cantilever and the mesh (DOFs = 130).

SBFEM reaches 18% with $\Delta t = 0.02\,\mathrm{s}$ and 13% with $\Delta t = 0.01\,\mathrm{s}$ at the beginning and the end of analysis, respectively, although it is low in the middle stage. In contrast, the present method successfully limited the error close to the target $\bar{\omega} = 1\%$ in all the time steps by varying the time increments between 0.002 s and 0.033 s, as shown in Fig. 11(b).

4.3. *Example 3: A deep cantilever under impact*

A deep cantilever subjected to a uniformly distributed loading in the form of Heaviside function on the top face (Fig. 12). The dynamic responses in (0, 30 s) were calculated.

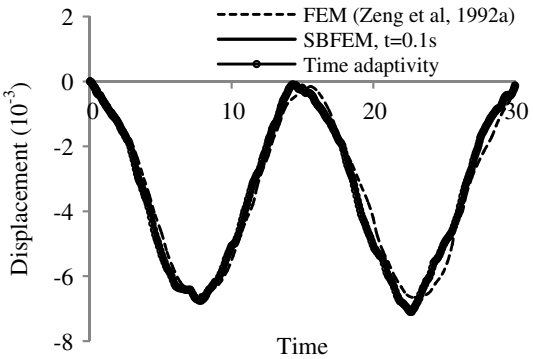

Fig. 13. Histories of vertical displacement of point A.

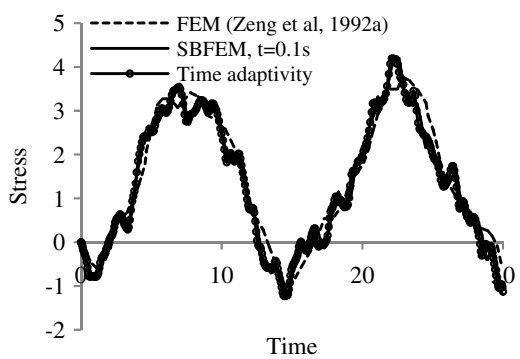

Fig. 14. Histories of horizontal stress of point B.

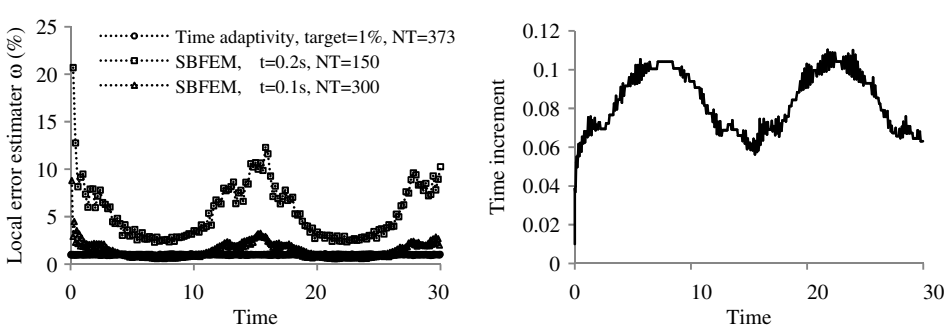

(a) (b)

Fig. 15. Histories of the local error estimator and the time increment for Example 3: (a) the local error estimator and (b) the time increment.

Figures 13 and 14 compare the histories of vertical displacement at point A and the horizontal stress at point B respectively, calculated by the present method, nonadaptive SBFEM, and FEM using 3,460 DOFs [Zeng and Wiberg (1992a)]. The results are in good agreement with each other. Figure 15(a) shows the histories of the local error estimator from the present method and nonadaptive SBFEM with time increments $\Delta t = 0.1\,\mathrm{s}$ and $\Delta t = 0.2\,\mathrm{s}$, respectively. Again, the present method successfully limited the error around the target although it used more time steps than the nonadaptive SBFEM. Figure 15(b) shows the history of the time increment used in the present method.

5. Conclusions

An adaptive time-stepping procedure based on the SBFEM has been developed for elastodynamic problems. The total energy of the domain is calculated semi-analytically. A local error estimator based on the assumption of linearly distributed acceleration is established to evaluate the time discretization error. The time increment is automatically identified to satisfy the pre-specified target error estimator. Numerical examples demonstrate that the developed method is able to accurately calculate dynamic responses and limit the time discretization error within acceptable levels, using a small number of DOFs.

Acknowledgments

This research is supported by EPSRC UK (Project No. EP/F00656X/1). Z. H. Zhang's one-year study in the University of Liverpool is funded by China Scholarship Council.

References

Deeks, A. J. and Wolf, J. P. [2002b] An h-hierarchical adaptive procedure for the scaled boundary finite-element method, *Int. J. Numer. Methods Eng.* **54**(4), 585–605.

Deeks, A. J. and Wolf, J. P. [2002a] Stress recovery and error estimation for the scaled boundary finite-element method, *Int. J. Numer. Methods Eng.* **54**(4), 557–583.

Ihlenburg, F., Babuska, I. and Sauter, S. [1997] Reliability of finite element methods for the numerical computation of waves, *Adv. Eng. Software* **28**, 417–424.

Li, X. D., Zeng, L. F. and Wiberg, N.-E. [1993] A simple local error estimator and an adaptive time-stepping procedure for direct integration method in dynamic analysis, *Commun. Numer. Methods Eng.* **9**, 273–292.

Song, C. and Wolf, J. P. [1997] The scaled boundary finite-element method — alias consistent infinitesimal finite-element cell method for elastodynamics, *Comput. Methods Appl. Mech. Eng.* **147**(3–4), 329–355.

Thomas, R. M. and Gladwell, I. [1988] Variable-order variable-step algorithms for second-order systems. Part 1: the methods, *Int. J. Numer. Methods Eng.* **26**(1), 39–53.

Voleti, S. R., Chandra, N. and Miller, J. R. [1996] Global-local analysis of large-scale composite structures using finite element methods, *Comput. Struct.* **58**(3), 453–464.

Yang, Z. J. [2006] Fully automatic modelling of mixed-mode crack propagation using scaled boundary finite element method, *Eng. Fract. Mech.* **73**(12), 1711–1731.

Yang, Z. J., Deeks, A. J. and Hao, H. [2007] Transient dynamic fracture analysis using scaled boundary finite element method: a frequency-domain approach, *Eng. Fract. Mech.* **74**(5), 669–687.

Yang, Z. J., Zhang, Z. H., Liu, G. H. and Ooi, E. T. [2011] An h-hierarchical adaptive scaled boundary finite element method for elastodynamics, *Comput. Struct.* **89**, 1417–1429.

Zeng, L. F. and Wiberg, N.-E. [1992a] Spatial mesh adaptive in semidiscrete finite element analysis of linear elastodynamic problems, *Comput. Mech.* **9**(5), 315–332.

Zeng, L. F., Wiberg, N.-E. and Bernspång, L. [1992b] An adaptive finite element procedure for 2D dynamic transient analysis using direct integration, *Int. J. Numer. Methods Eng.* **34**(3), 997–1014.

Zeng, L. F., Wiberg, N.-E., Li, X. D. and Xie, Y. M. [1992c] *A posteriori* local error estimation and adaptive time-stepping for Newmark integration in dynamic analysis, *Earthquake Eng. Struct. Dyn.* **21**, 555–571.

Zienkiewicz, O. C. and Xie, Y. M. [1991] A simple error estimator and adaptive time stepping procedure for dynamic analysis, *Earthquake Eng. Struct. Dyn.* **20**, 871–887.

Zienkiewicz, O. C. and Zhu, J. Z. [1987] A simple error estimator and adaptive procedure for practical engineering analysis, *Int. J. Numer. Methods Eng.* **24**(2), 337–357.